Ice Polar Stratospheric Clouds Detected from Assimilation of Atmospheric Infrared Sounder Data

Ivanka Stajner,[1,2] Craig Benson,[3,2] Hui-Chun Liu,[1,2] Steven Pawson,[2] Nicole Brubaker,[1,2] Lang-Ping Chang,[1,2] Lars Peter Riishojgaard[3,2], and Ricardo Todling[1,2]

[1] Science Applications International Corporation, Beltsville, Maryland
[2] Global Modeling and Assimilation Office, NASA Goddard Space Flight Center, Greenbelt, Maryland
[3] Goddard Earth Sciences and Technology Center, University of Maryland Baltimore County, Baltimore, Maryland

A novel technique is presented for the detection and mapping of ice polar stratospheric clouds (PSCs), using brightness temperatures from the Atmospheric Infrared Sounder (AIRS) "moisture" channel near 6.79 µm. It is based on observed-minus-forecast residuals (O-Fs) computed when using AIRS radiances in the Goddard Earth Observing System version 5 (GEOS-5) data assimilation system. Brightness temperatures are computed from six-hour GEOS-5 forecasts using a radiation transfer module under clear-sky conditions, meaning they will be too high when ice PSCs are present. We study whether the O-Fs contain quantitative information about PSCs by comparison with sparse data from the Polar Ozone and Aerosol Measurement (POAM) III solar occultation instrument. AIRS O-Fs lower than –2 K generally coincide with PSCs observed by POAM III. Synoptic maps of AIRS O-Fs lower than –2 K are constructed as a proxy for ice PSCs. These are used to investigate spatio-temporal variations of Antarctic PSCs in the year 2004.

1. Introduction

Polar stratospheric clouds (PSCs) form at extremely low temperatures in the lower stratosphere during Antarctic and Arctic winters. PSCs provide surfaces for heterogeneous chemical reactions leading to subsequent ozone destruction (e.g. Solomon 1999). The abundance of PSCs is determined by the climate and its variability through a very strong dependence on temperature. Their presence controls polar ozone loss, which in turn has a cooling effect on the climate.

Most satellite observations of PSCs have been made by occultation or limb sounding instruments with sparse horizontal coverage. They can provide quite detailed information on the vertical distribution and composition of PSCs (e.g. Fromm et al. 1997; Poole et al. 2003; Spang et al. 2005; Höpfner et al. 2006).

Data from nadir-viewing instruments like TOVS HIRS2 and the Advanced Very High Resolution Radiometer (AVHRR) have provided information about ice PSCs (Meerkoetter 1992; Hervig et al. 2001). Maps of ice PSCs were retrieved from differences in radiances in two channels and also allowed distinction between ice PSCs and cirrus. In contrast, even the strongest nitric-acid-trihydrate PSCs cannot be retrieved from AVHRR because their signal falls below AVHRR measurement uncertainty (Hervig et al. 2001).

Tropospheric ice clouds can be retrieved from the Atmospheric Infrared Sounder (AIRS) data. Comparisons of AIRS spectra with a radiative transfer model in the window region 10-12.5 µm show signatures of near-micron sized cirrus ice particles (Kahn et al. 2003). Cirrus decreases brightness temperatures in the moisture channels around 7 µm, independently of the aerosol conditions below the cloud (Hong et al. 2006).

AIRS brightness temperatures are among the observations included in the Goddard Earth Observing System version 5 (GEOS-5) data assimilation system. We study differences between AIRS observations that are influenced by clouds and simulated brightness temperatures from GEOS-5 that are calculated under cloud-free conditions. The size of these observed-minus-forecast residuals (O-Fs) will be shown to correlate with the presence of ice PSCs in collocated data from the Polar Ozone and Aerosol Measurement (POAM) III instrument. The high spatial density of AIRS data is then used to construct maps of ice PSCs and evaluate their spatial and temporal variability.

2. AIRS data

AIRS is a high-resolution spectrometer, with 2378 spectral channels between 3.74 and 15.4 µm (e.g., Aumann et al. 2003). Atmospheric temperature, composition, and cloudiness can be retrieved from AIRS measurements (Susskind et al. 2006). AIRS is one of six instruments on board NASA's Aqua platform, which flies in a 1:30PM ascending-node orbit with an inclination of 98° at an altitude of 705 km. AIRS provides high spatial data density from 1650 km wide swaths with a nadir footprint of 13.5 km. In polar regions, where the orbits converge, the off-nadir soundings yield information at a variety of synoptic times. Vertical information on thermal structure and composition is limited by the physical constraints on averaging kernels for near-nadir sounders.

The analysis presented in this paper focuses on the 6.79-μm moisture channel. Emission from near 200 hPa provides the peak contribution to this channel. There is very little sensitivity to the surface and the lower troposphere, even under cold and dry Antarctic winter conditions (Fig. 1). Radiative transfer model simulations under Antarctic conditions indicate that this channel is sensitive to ice clouds at altitudes above the weighting function peak in the colder stratosphere. Simulated brightness temperature is lower when presence of an ice PSC is assumed than under clear-sky conditions, indicating a possibility for detection of ice PSCs using this channel. Other methods for cirrus or PSC detection from infrared radiances use surface-sensitive window channels and rely on the contrast between a warm surface and a cold cloud top, which limits their applicability over the frozen Antarctic continent (Hervig et al. 2001; Kahn et al. 2003; Wei et al. 2004).

3. Assimilation system

In GEOS-5, observations are assimilated into the general circulation model using Gridpoint Statistical Interpolation (GSI, Wu et al. 2002). The interface between GSI and the model uses Incremental Analysis Update (Bloom et al. 1996). The community radiative transfer model (CRTM) provides the AIRS observation operator within GSI (Weng and Liu 2003). The present version of CRTM models clear-sky conditions, producing typically negative AIRS O-Fs over clouds.

AIRS data volume in the assimilation is reduced by selection of 152 channels, which are a subset of the 281 channels used by Le Marshal et al. (2006). AIRS data are thinned spatially by selecting the scan with the warmest brightness temperature in the window channel near 10.36 μm (i.e. observations that are the least affected by clouds) in each 180km×180km box. Even though thinned AIRS data are assimilated, the O-Fs in this study are shown without spatial thinning. GEOS-5 was run at 1° latitude by 1.25° longitude resolution with 72 levels between the surface and 0.01 hPa.

4. Comparisons with POAM data

Ice PSC data from POAM instruments are well studied (Fromm et al. 1997). POAM provides sparse solar occultation data from a single latitude in each hemisphere in one day. Ice PSCs are detected when a downward occultation scan terminates at least 3 km above the tropopause, when large opacity of a PSC reduces the solar radiance to levels below the tracking threshold. Data from POAM III are used here to infer the criteria for PSC signatures in AIRS O-Fs.

A map of AIRS 6.79 μm brightness temperature O-Fs (Fig. 2) reveals many values within ±1 K, denoted by light shades of orange. At the latitude where POAM observed, detected ice clouds (circles) coincide with lower AIRS O-F residuals (blue), and locations without ice PSCs coincide with higher AIRS O-F residuals (orange). POAM scans that terminate between 2 and 3 km above the tropopause are marked separately, because a cloud is present, but there is ambiguity whether the cloud top is in the stratosphere or the troposphere. POAM data collected over 24 h are shown. The AIRS O-Fs are shown for the four synoptic times, closest to POAM measurement time in each quadrant. As expected, the agreement between POAM data and AIRS O-Fs is better in the regions where O-Fs are more uniform. Smaller scale variability in O-Fs together with several hours of difference between AIRS and POAM overpasses introduce some discrepancies (in this case near 130°E and 300°E).

The time series of POAM data and collocated AIRS O-Fs (within 200 km and 6 h) in August and September 2004 is shown in Fig. 3. AIRS O-Fs are often lower than –2 K in the presence of ice PSCs in POAM data, and higher than –2 K in the absence of ice PSCs. This distinction is more clear for measurements taken within 2 h (red and orange marks). The scatter in O-Fs increases with larger time differences between POAM and AIRS measurements, which is expected due to inhomogeneity of clouds. The time difference between POAM and AIRS is generally larger in August (when POAM measures near 11 am local time) than in September (when POAM measures in late afternoon). Differences in AIRS and POAM measurement times, horizontal resolutions and viewing geometry (see Kahn et al 2002), errors in GEOS-5 forecasts (e.g. in upper tropospheric moisture), presence of cirrus clouds, and measurement errors can all contribute to the scatter.

Comparisons with POAM data support the hypothesis that AIRS O-Fs for the 6.79-μm channel that are lower than –2 K indicate the presence of ice PSCs.

5. Distribution of ice PSCs

In this section distributions of ice PSCs are inferred from AIRS 6.79-μm O-Fs lower than –2 K. In September, their occurrence is most prevalent between about 70°S and the South Pole, near 315°E, which is to the east of the Antarctic peninsula (Fig. 4a). This location agrees with the location of high frequency of

PSCs in POAM II observations and in earlier climatologies (Fromm et al. 1997 and references therein). Topographic gravity waves originating from the Antarctic peninsula contribute to formation of PSCs in this region (Cariolle et al. 1989).

In August, two regions show enhanced presence of O-Fs lower than –2 K: east of the Antarctic peninsula, and over the high terrain near 100°E (Fig. 4b). The maximum near 100°E is not present in the Fromm et al. (1997) seasonal climatology, which is based on detection of any type of PSCs by POAM II for years 1994-1996 and includes only ice PSCs detected above 17 km altitude. Each of these conditions may contribute to the differences in the distribution of PSCs in longitude. In support of our finding of maximum frequency near 100°E, note that POAM II data in August 1995 show a strong mode in the PSC frequency near 120°E (*op. cit.*).

Longitudinal structure in PSCs can arise from temperature perturbations associated with synoptic scale waves (Tuck, 1989). Data from two Antarctic stations, Syowa (69°S, 40°E) and Davis (69°S, 78°E), demonstrate a correlation between these phenomena (Shibata et al., 2003; Innis and Klekociuk 2006).

The Antarctic middle stratosphere (near 22 km altitude) was warmer than usual in 2004, with the smallest ozone depletion in August among years 1994-1996 and 1998-2004 (Hoppel et al., 2005). However, temperature soundings at the South Pole indicate typical conditions between about 10 and 14 km altitude, and even colder than usual near 8 km at Neumayer (70°S, 352°E). Cold temperatures in the upper troposphere and lower stratosphere (UT/LS) allow formation of ice clouds. Some clouds are in the stratosphere according to the POAM data (e.g between 0°E and 100°E in Fig. 2), but tropospheric clouds with cloud tops at the tropopause cannot be ruled out (e.g. near 350°E in Fig. 2).

Vertical motion in the UT/LS at 200 hPa shows strongest upwelling near 90°E and 280°E, with downwelling near 0°E and 150°E (Fig. 5). The coldest temperatures extend near 110°E. Thus, high frequency of the ice clouds in Fig. 4b corresponds to the upwelling in a cold region.

6. Discussion and conclusions

Assimilation of AIRS radiances in GEOS-5 provides a novel technique for detection of ice clouds in the Antarctic stratosphere. We found that those O-F residuals for AIRS moisture channel near 6.79 μm that are lower than –2K typically coincide with POAM III observations of ice PSCs (Fig. 3). The high horizontal resolution of AIRS enables creation of synoptic ice PSC maps (Fig. 2), which can be used for study of PSC frequency (Fig. 4) and variability.

Spatial distribution of ice PSCs inferred from O-F residuals in September 2004 agrees with a previous climatology. The distribution in August is quite different, with high frequency of clouds near 100°E. POAM data and GEOS-5 meteorological fields support frequent ice clouds in that region, but some of them may be cirrus clouds. Coarser resolution of POAM near the tropopause does not allow definitive distinction between PSCs and cirrus. In addition, PSCs are often found in cold regions above cirrus clouds, which shield radiation from the warmer troposphere below. Observations of PSCs extending from the tropopause to 21 km altitude (Palm et al. 2005), together with frequent upwelling near the tropopause in August of 2004 suggest a possibility of localized lofting along the trajectories of moist tropospheric air masses and formation of ice clouds as they saturate in the stratosphere.

Some of the scatter in the comparisons of AIRS and POAM data (Fig. 3) is likely due to differences in their measurement times. Data from recently launched CALIPSO lidar (Heymsfield et al. 2005), which is coincident with AIRS within a couple of minutes will be used in future comparisons to better characterize the sensitivity of AIRS O-Fs to ice PSCs and cirrus clouds.

Assimilation of AIRS radiances improves numerical weather forecasting (McNally et al. 2006; Le Marshal et al. 2006). Better understanding of signatures of PSC and cirrus clouds in the AIRS data could potentially improve impacts of AIRS on weather forecasting.

Acknowledgements

We thank NASA Modeling and Analysis Program for support.

References

Aumann, H. H., et al., AIRS/AMSU/HSB on the Aqua Mission: Design, science objectives, data products, and processing systems, IEEE Trans. Geosci. Remote Sens., 41(2), 253–264, 2003.

Bloom, S. C., L. L. Takacs, A. M. da Silva, and D. Ledvina (1996), Data Assimilation Using Incremental Analysis Updates, *Mon. Weather Rev.,* 124, 1256-1271.

Cariolle, D., S. Muller, F. Cayla, and M. P. McCormick (1989), Mountain waves, polar stratospheric clouds, and the ozone depletion over Antarctica, *J. Geophys. Res.*, 94(D9), 11,233–11,240.

Fromm, M. D., J. D. Lumpe, R. M. Bevilacqua, E. P. Shettle, J. Hornstein, S. T. Massie, and K. H. Fricke (1997), Observations of Antarctic polar stratospheric clouds by POAM II: 1994–1996, *J. Geophys. Res.*, 102(D19), 23,659–23,673.

Hervig, M. E., K. L. Pagan, and P. G. Foschi, Analysis of PSC measurements from AVHRR, J. Geophys. Res., 106(D10), 10,363 –10,374, 2001

Heymsfield, A. J., D. Winker, and G.-J. van Zadelhoff (2005), Extinction-ice water content-effective radius algorithms for CALIPSO, *Geophys. Res. Lett.*, 32, L10807, doi:10.1029/2005GL022742.

Höpfner, M. et al., MIPAS detects Antarctic stratospheric belt of NAT PSCs caused by mountain waves, Atmos. Chem. Phys., 6, 1221–1230, 2006.

Hong, G., P. Yang, H.-L. Huang, S. A. Ackerman, and I. N. Sokolik (2006), Simulation of high-spectral-resolution infrared signature of overlapping cirrus clouds and mineral dust, *Geophys. Res. Lett.*, 33, L04805, doi:10.1029/2005GL024381.

Hoppel, K., G. Nedoluha, M. Fromm, D. Allen, R. Bevilacqua, J. Alfred, B. Johnson, and G. König-Langlo (2005), Reduced ozone loss at the upper edge of the Antarctic Ozone Hole during 2001–2004, *Geophys. Res. Lett.*, 32, L20816, doi:10.1029/2005GL023968.

Innis, J. L., and A. R. Klekociuk (2006), Planetary wave and gravity wave influence on the occurrence of polar stratospheric clouds over Davis Station, Antarctica, seen in lidar and radiosonde observations, *J. Geophys. Res.*, 111, D22102, doi:10.1029/2006JD007629.

Kahn, B.h., A. Eldering, F. W. Irion, F. P. Mills, B. Sen, and M. R. Gunson, Cloud identification in Atmospheric Trace Molecule Spectroscopy infrared occultation measurements, Aplied Optics, 41, 2768-2780.

Kahn, B. H., A. Eldering, S. A. Clough, E. J. Fetzer, E. Fishbein, M. R. Gunson, S. Lee, P. F. Lester, and V. J. Realmuto (2003), Near micron-sized cirrus cloud particles in high-resolution infrared spectra: An orographic case study, *Geophys. Res. Lett.*, 30(8), 1441, doi:10.1029/2003GL016909.

Le Marshall J, Jung J, Derber J, et al., Improving Global Analysis and Forecasting with AIRS, *Bull. Am. Met. Soc.*, 87 (7), doi:10.1175/BAMS-87-7-891, 2006.

McNally AP, Watts PD, Smith JA, Engelen R, Kelly GA, Thepaut JN, Matricardi M (2006), The assimilation of AIRS radiance data at ECMWF, *Q. J. R. Meteorol. Soc.,* 132, 935-957.

Meerkoetter R., Detection of polar stratospheric clouds from NOAA-HIRS data: a case study, Geophys. Res. Lett., Vol. 19, No.13, pp. 1351-1354, 1992.

Palm, S. P., M. Fromm, and J. Spinhirne (2005), Observations of antarctic polar stratospheric clouds by the Geoscience Laser Altimeter System (GLAS), *Geophys. Res. Lett.*, 32, L22S04, doi:10.1029/2005GL023524.

Poole, L. R., C. R. Trepte, V. L. Harvey, G. C. Toon, and R. L. VanValkenburg, SAGE III observations of Arctic polar stratospheric clouds – December 2002, Geoph. Res. Lett., VOL. 30, NO. 23, 2216, doi:10.1029/2003GL018496, 2003.

Shibata, T., K. Sato, H. Kobayashi, M. Yabuki, and M. Shiobara (2003), Antarctic polar stratospheric clouds under temperature perturbation by nonorographic inertia gravity waves observed by micropulse lidar at Syowa Station, *J. Geophys. Res.*, 108(D3), 4105, doi:10.1029/2002JD002713.

Spang, R., Remedios, J. J., Kramer, L. J., Poole, L. R., Fromm, M. D., Müller, M., Baumgarten, G., and Konopka, P.: Polarstratospheric cloud observations by MIPAS on ENVISAT: detection method, validation and analysis of the northern hemisphere winter 2002/2003, Atmos. Chem. Phys., 5, 679–692, 2005.

Susskind, J., C. Barnet, J. Blaisdell, L. Iredell, F. Keita, L. Kouvaris, G. Molnar, and M. Chahine (2006), Accuracy of geophysical parameters derived from Atmospheric Infrared Sounder/Advanced Microwave Sounding Unit as a function of fractional cloud cover, *J. Geophys. Res.*, 111, D09S17, doi:10.1029/2005JD006272.

Tuck, A. F. (1989), Synoptic and chemical evolution of the Antarctic vortex in late winter and early spring, 1987, *J. Geophys. Res.*, 94(D9), 11,687–11,737.

Wei HL, Yang P, Li J, Baum BA, Huang HL, Platnick S, Hu YX, Strow L (2004), Retrieval of semitransparent ice cloud optical thickness from atmospheric infrared sounder (AIRS) measurements, *IEEE Trans. Geosci. Remote Sens.,* 42 (10): 2254-2267.

Weng, F. and Q. Liu (2003), Satelite data assimilation in numerical weather prediction models. Part 1: Forward radiative transfer and Jacobian models under cloudy conditions, *J. Atmos. Sci.,* 60, 2633-2646.

Wu, W.-S., R. J. Purser, and D. F. Parish (2002), Three-dimensional variational analyses with spatially inhomogeneous covariances, *Mon. Wea. Rev.,* 130, 2905-2916.

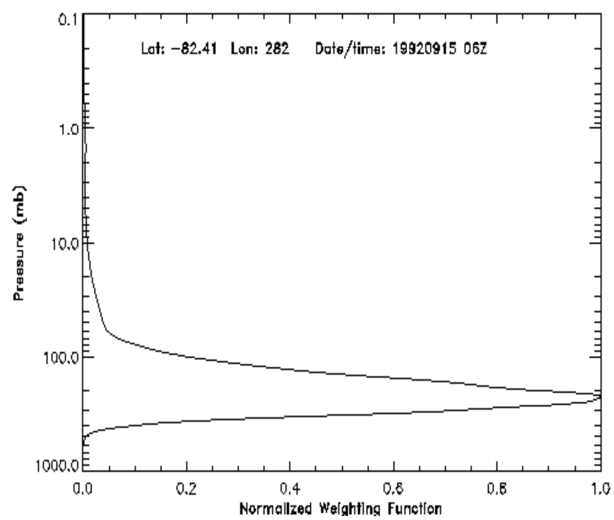

Figure 1. Normalized weighting function for the AIRS 6.79-μm channel at an Antarctic location in September.

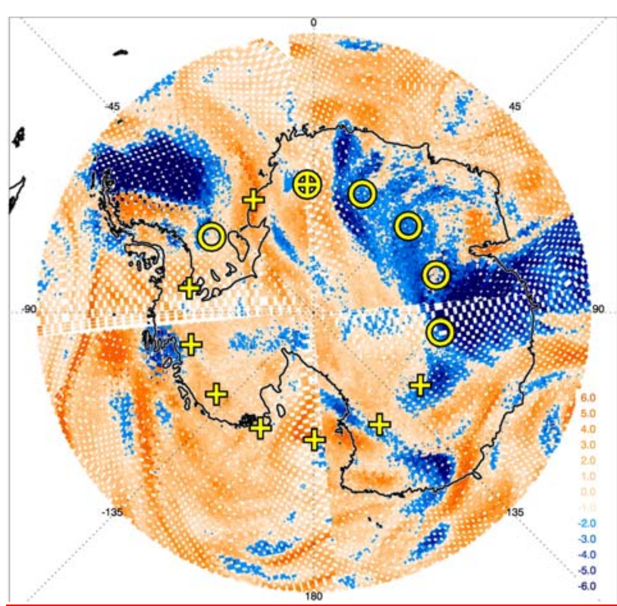

Figure 2. A composite map of AIRS O-Fs in K (color) for the 6.79-µm channel on August 18, 2004. POAM data for that day are marked by the presence of ice PSCs (circle), absence of ice PSCs (plus sign), or presence of a cloud in the immediate vicinity of the tropopause (plus inside a circle, see text for details). In each quadrant AIRS O-Fs for the synoptic time closest to the POAM measurement time are shown for the region south of 60°S. Greenwich meridian points towards the top of the figure.

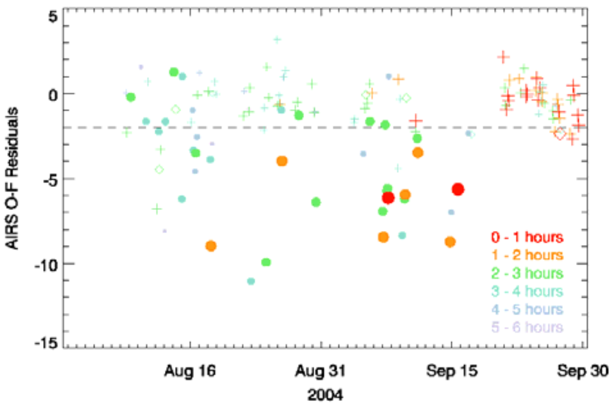

Figure 3. Comparison of AIRS O-Fs with POAM data within 200 km in August and September 2004. Color indicates time difference between POAM and AIRS measurements. POAM profiles with ice PSCs (•) correspond to lower AIRS O-Fs than POAM profiles without ice PSCs (+). Separation of O-F residuals with respect to –2 K (dashed) is more clear for smaller time differences between POAM and AIRS (red, orange), than for larger ones (blue, green). POAM detection of clouds near the tropopause is marked (◊).

a)

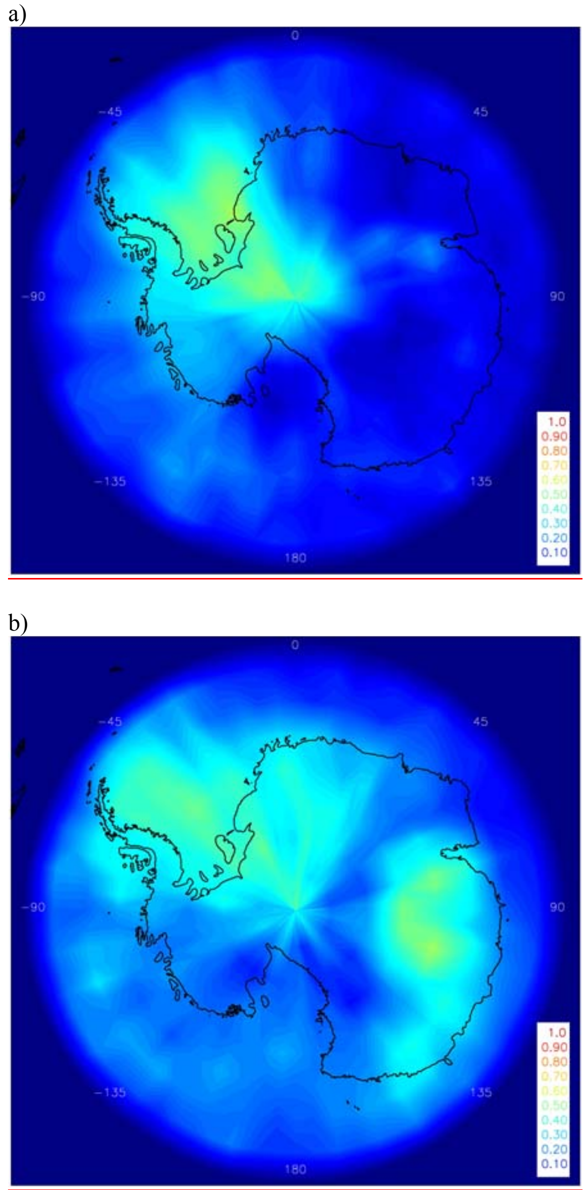

b)

Figure 4. Maps of the relative frequency of AIRS O-Fs lower than –2 K for the 6.79-µm channel computed for all available data in a) September and b) August 2004.

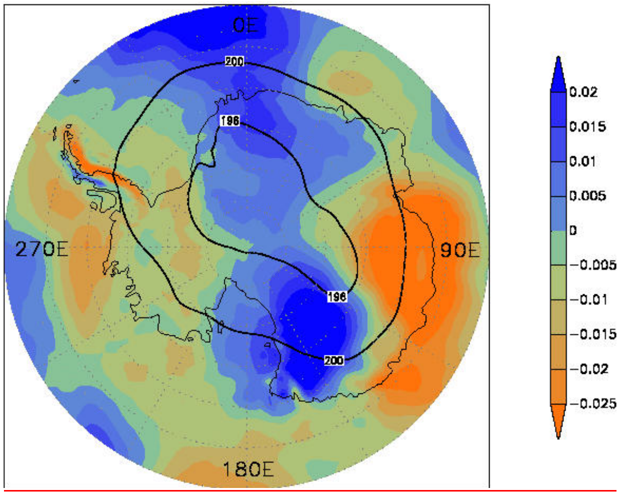

Figure 5. Map of the monthly averaged vertical velocity ω in Pa/s (color) and temperature in K (contours) at 200 hPa in August 2004 from GEOS-5.